

Original Research

# Quercetin/Anti-PD-1 Antibody Combination Therapy Regulates the Gut Microbiota, Impacts Macrophage Immunity and Reshapes the Hepatocellular Carcinoma Tumor Microenvironment

Ruoxia Wu<sup>1,\*</sup>, Jiaqing Xiong<sup>2</sup>, Ting Zhou<sup>3</sup>, Zhen Zhang<sup>4</sup>, Zhen Huang<sup>5</sup>, Sha Tian<sup>5</sup>, Yongli Wang<sup>6</sup><sup>1</sup>School of Traditional Chinese Medicine, Hunan University of Chinese Medicine, 410208 Changsha, Hunan, China<sup>2</sup>Teaching and Research Section of Traditional Chinese Medicine Surgery, The First Hospital of Hunan University of Chinese Medicine, 410021 Changsha, Hunan, China<sup>3</sup>School of Pharmacy, Hunan University of Chinese Medicine, 410208 Changsha, Hunan, China<sup>4</sup>Department of Oncology, the Affiliated Hospital of Hunan Academy of Traditional Chinese Medicine, 410006 Changsha, Hunan, China<sup>5</sup>College of Integrated Traditional Chinese and Western Medicine, Hunan University of Chinese Medicine, 410208 Changsha, Hunan, China<sup>6</sup>Department of Oncology, The First Hospital of Hunan University of Chinese Medicine, 410021 Changsha, Hunan, China\*Correspondence: [004329@hnuqm.edu.cn](mailto:004329@hnuqm.edu.cn) (Ruoxia Wu)

Academic Editor: Gianfranco Alpini

Submitted: 24 March 2023 Revised: 3 May 2023 Accepted: 16 May 2023 Published: 1 December 2023

## Abstract

**Objective:** The use of immune checkpoint inhibitors (ICIs) provides promising strategies for hepatocellular carcinoma (HCC) treatment. This study aimed to explore impact and underlying mechanism of the combination therapy of quercetin and anti-programmed cell death 1 (anti-PD-1) antibody on HCC. **Methods:** Orthotopically transplanted HCC tumors in mice were treated with quercetin, anti-PD-1 antibody, or a combination of both therapies. Histopathological changes and programmed cell death ligand 1 (PD-L1) expression were characterized by hematoxylin and eosin (H&E) and immunohistochemistry (IHC) staining. The diversity and differences of gut microbiota (GM) were evaluated through 16S rRNA sequencing. Levels of macrophage immunity-related cytokines were quantified by enzyme-linked immunosorbent assay (ELISA), quantitative real-time polymerase chain reaction (RT-qPCR), and Western blot. **Results:** Combination therapy reduced necrosis, fibrosis, and PD-L1 expression in liver tissues. Additionally, combination therapy reduced GM imbalance and increased abundance of *Firmicutes*, *Actinobacteria*, and *Verrucomicrobiota* at the phylum level as well as *Dubosiella* and *Akkermansia* at the genus level. Combination therapy improved macrophage immunity, raised the expressions of CD8a, CD4, CD11b, interleukin (IL)-10, and interferon (IFN)- $\gamma$ , and declined the expressions of IL-4, IL-6, toll-like receptor 4 (TLR4), an inhibitor of nuclear factor  $\kappa$ B $\alpha$  (*I $\kappa$ B $\alpha$* ), and the NF $\kappa$ B subunit p65. Upon combination therapy, expressions of M2 macrophage-related genes arginase-1 (*Arg-1*), *IL-10*, transforming growth factor- $\beta$  (*TGF- $\beta$* ), and matrix metalloproteinase-9 (*MMP-9*) were upregulated. Instead, M1 macrophage-related genes *IL-6*, *IL-12a*, *IL-1 $\beta$* , and tumor necrosis factor- $\alpha$  (*TNF- $\alpha$* ) were downregulated. **Conclusions:** Quercetin/anti-PD-1 antibody combination therapy reshaped HCC tumor microenvironment in mice in parallel with regulating the GM and macrophage immunity.

**Keywords:** quercetin; anti-PD-1 antibody; hepatocellular carcinoma; gut microbiota; macrophage immunity

## 1. Introduction

Hepatocellular carcinoma (HCC) is a malignant tumor that arises in hepatocytes. HCC is the most common pathological type of primary liver cancer and a principal cause of cancer-related deaths globally [1]. Clinically, surgery is the most effective treatment for HCC and includes both hepatectomy and liver transplantation). However, most HCC patients frequently miss the opportunity to have surgery due to the poor rate of early disease diagnosis [2]. Therefore, research into HCC diagnosis and innovative treatments is a critical step to improving response to this form of cancer.

Transcriptome analysis has revealed a marked local upregulation of both programmed cell death 1 (PD-1) and programmed cell death 1 ligand 1 (PD-L1) in the tumor microenvironment (TME) of HCC. FoxP3-positive

lymphocytic infiltration, E-cadherin deficiency, epithelial-mesenchymal transition (EMT), and an extremely poor histologic differentiation are also observed [3]. Immune checkpoint blockade immunotherapy resulted in the activation of the nuclear factor kappa B (NF- $\kappa$ B) pathway in tumor-associated macrophages (TAMs). This event occurred through toll-like receptor 2 (TLR2) and myeloid differentiation factor 88 (MyD88), and a recruitment of p62 to activate the autophagy-related pathways. Moreover, exogenous intervention resensitized the response of tumor-local T cells to anti-PD-1 immunotherapy [4]. Hence, the approach of using PD-1 blockers to modulate TAMs within the TME, and removing T-cell inhibitory signals to exert a synergistic anti-tumor effect offers a promising approach for HCC treatment.



Previous findings have indicated that PD-L1 and gut microbiota may serve as potential predictive biomarkers for immunotherapy responses in the case of advanced HCC [5,6]. Recent studies have increasingly demonstrated that gut microbiota (GM) can affect the occurrence and progression of HCC through the gut-liver axis [7]. Cooperation between GM and immune checkpoint inhibitors (ICIs) has particularly improved the effectiveness of PD-1 blockade therapy for cancers [8]. As such, GM may play a critical role in the response of HCC patients who are treated with an anti-PD-1 immunotherapy regimen [9]. Research on the combination of ICIs and other drugs or therapies for the treatment of malignant tumors has been reported [10,11]. Quercetin is characterized as an effective liver protector due to its antioxidant, anti-inflammatory, and anti-cancer activities [12]. Its therapeutic effects on HCC have been studied both *in vitro* and *in vivo* models [13]. Further, quercetin has been demonstrated as an alternative therapy for preventing HCC early in the process of tumorigenesis by regulating key TME components [14]. Prior research has shown that quercetin, functioning as a cancer chemopreventive agent, can attenuate the inhibition of PD-L1 on T lymphocytes by altering the PD-1/PD-L1 interaction [15]. However, the combination therapy of quercetin and anti-PD-1 immunotherapy on GM and TME in HCC requires further exploration.

In this study, we used an orthotopically transplanted HCC mouse model that was treated with quercetin, anti-PD-1 antibody, or a combination therapy. We explored the impact of the combination therapy on GM and macrophage immunity in HCC mice as a means to provide new insights for the application of traditional Chinese medicine (TCM) and immunotherapy in HCC.

## 2. Materials and Methods

### 2.1 Construction of an Orthotopically Transplanted HCC Mouse model and Intervention Treatment

Male 8-week-old C57L/J mice were obtained from Hunan Slyke Jingda Laboratory Animal Co., Ltd (Changsha, China). The construction of an orthotopically transplanted HCC model was performed following one week of adaption [16]. Briefly,  $1 \times 10^6$  Hepal-6 cells were subcutaneously injected into the right axilla. When the tumor grew to a volume of 1–2 cm<sup>3</sup>, it was harvested and cells cultured. The fourth generation of cells were selected for the orthotopically transplanted HCC model used in this investigation. Following anesthesia (10% chloral hydrate, 0.3 mL/100 g), the livers of mice were exposed and  $1 \times 10^6$  fourth-generation Hepal-6 cells were directly seeded into the left lobe of the liver and compressed with a gelatin sponge for hemostasis. Mice in the Control group were subjected to all surgical procedures except without injection of Hepal-6 cells.

The experimental treatment groups were listed as follows: Control, Model, Quercetin, anti-PD-1, and

Quercetin+anti-PD-1, and each group contained 8 mice. The corresponding intervention was administered to mice 14 days after cell implantation. Mice in the Control and Model groups were gavaged with the same dose of distilled water for 14 days. Mice in the Quercetin group were gavaged daily with quercetin (100 mg/kg-d, Q817162, Macklin, Shanghai, China) for 14 days [17]. Mice in the anti-PD-1 group were injected with anti-PD-1 antibody (20 mg/kg, B276435, Aladdin, Shanghai, China) through the tail vein twice a week for 14 days [18]. Mice in the Quercetin+anti-PD-1 group received both treatments as outlined above simultaneously for 14 days. On day 28 after cell implantation, the mice were sacrificed, and blood, livers, and feces were collected. Livers were fixed with 4% paraformaldehyde followed by embedding in paraffin, and subsequently sectioned for staining analysis.

### 2.2 Hematoxylin and Eosin Staining

The liver tissue slices were first dewaxed by placing them in xylene for 20 min followed by dehydration with an ethanol gradient (75–100%). After this, the slices were stained with hematoxylin (AWI0001a, Abiowell, Changsha, China) for 1–10 min and subsequently rinsed in phosphate buffer saline (PBS). Afterward, the slices were stained with eosin (AWI0029a, Abiowell) for 1–5 min, washed with distilled water, and then dehydrated with an ethanol gradient (95–100%). Finally, the slices were placed in xylene for 10 min for tissue transparency and sealed with neutral gum (AWI0238a, Abiowell) prior to observation.

### 2.3 Quantitative Real-Time Polymerase Chain Reaction

Total RNA was extracted from liver tissues using Trizol reagent (15596026, Thermo, Waltham, MA, USA). Following this, mRNA was reverse transcribed into cDNA using a reverse transcription kit (CW2569, CWBIO, Beijing, China), followed by quantitative real-time polymerase chain reaction (RT-qPCR). The primers were as follows: *β-actin*: F: 5'-ACATCCGTAAGACCTCTATGCC-3', R: 5'-TACTCCTGCTTGCTGATCCAC-3'; interleukin-6 (*IL-6*): F: 5'-GACTTCCATCCAGTTGCCTT-3', R: 5'-ATGTGTAATTAAGCCTCCGACT-3'; *IL-12a*: F: 5'-TGAAGACATCACACGGGACCA-3', R: 5'-CAGCTCCCTCTTGTGTGGAA-3'; *IL-1β*: F: 5'-TGCCACCTTTTGACAGTGATG-3', R: 5'-AAGGTCCACGGGAAAGACAC-3'; tumor necrosis factor- $\alpha$  (*TNF- $\alpha$* ): F: 5'-AGCACAGAAAGCATGATCCG-3', R: 5'-CACCCCGAAGTTCAGTAGACA-3'; arginase-1 (*Arg-1*): F: 5'-GGGCACACTCATGCATTCCT-3', R: 5'-GCGTCAGCTGCGAGTACATA-3'; *IL-10*: F: 5'-GTTCCCTACTGTTCATCCCC-3', R: 5'-AGGCAGACAAACAATACACCA-3'; transforming growth factor- $\beta$  (*TGF- $\beta$* ): F: 5'-CTCCCGTGGCTTCTAGTGC-3', R: 5'-GCCTTAGTTTGGACAGGATCTG-3'; ma-

trix metalloproteinase-9 (*MMP-9*): F: 5'-GCCCTGGAAGTACACGACA-3', R: 5'-GTAGCCCACGTCGTCCACC-3'. The relative gene expression level was calculated using the  $2^{-\Delta\Delta Ct}$  method with  $\beta$ -actin used as the internal reference.

#### 2.4 Western Blot

Liver tissues from different groups of mice were suspended in radio-immunoprecipitation assay (RIPA) lysate (AWB0136, Abiowell) to obtain total protein extracts. After separation by sodium dodecyl-sulfate polyacrylamide gel electrophoresis (SDS-PAGE), proteins were transferred onto the nitrocellulose (NC) membranes. After blocking with 5% skimmed milk (AWB0004, Abiowell) for 1.5 h, the NC membranes were incubated with primary antibodies at 4 °C overnight separately. Primary antibodies were as followed: CD8a (1:1000, ab33786, Abcam, Cambridge, UK), CD4 (1:1000, 19068-1-AP, Proteintech, Chicago, IL, USA), CD11b (1:1000, ab133357, Abcam), glyceraldehyde-3-phosphate dehydrogenase (GAPDH, 1:5000, 10494-1-AP, Proteintech), toll-like receptor 4 (TLR4, 1:1000, 19811-1-AP, Proteintech), inhibitor of nuclear factor  $\kappa$ B $\alpha$  (*I $\kappa$ B $\alpha$* , 1:2000, 10268-1-AP, Proteintech, Chicago, IL, USA), p-*I $\kappa$ B $\alpha$*  (1:10000, ab133462, Abcam), p-p65 (1:1000, ab76302, Abcam), p65 (1:5000, ab16502, Abcam), and  $\beta$ -actin (1:5000, 66009-1-Ig, Proteintech). The NC membranes were subsequently incubated with horseradish peroxidase (HRP)-goat anti-mouse IgG (1:5000, SA00001-1, Proteintech) or HRP-goat anti-rabbit IgG (1:6000, SA00001-2, Proteintech) for 1.5 h. Finally, the NC membranes were incubated with ECL reagent (AWB0005, Abiowell) and followed by chemiluminescent imaging. The expression levels of proteins were analyzed by Quantity One 4.6.6 software (Bio-Rad Inc., Hercules, CA, USA) using GAPDH or  $\beta$ -actin as the reference.

#### 2.5 Enzyme-Linked Immunosorbent Assay

For the detection of IL-6 (KE10007, Proteintech), IL-10 (KE10008, Proteintech), interferon- $\gamma$  (IFN- $\gamma$ , KE10001, Proteintech), and IL-4 (KE10010, Proteintech). Briefly, whole blood was placed for 2 h at room temperature followed by centrifugation at 1000 g for 15 min at 4 °C, and the supernatant was taken for analysis. For the detection of granulocyte-macrophage colony-stimulating factor (GM-CSF, KE10015, Proteintech, Chicago, IL, USA) and granulocyte colony-stimulating factor (G-CSF, KE10025, Proteintech), liver tissue was washed with PBS and homogenized, then placed at -20 °C overnight. After freeze-thaw treatment, the homogenate was centrifuged at 5000 g for 5 min at 4 °C, and then the supernatant was taken for analysis.

#### 2.6 Immunohistochemistry Staining

The liver slices were dewaxed by soaking in xylene for 20 min. Subsequently, dehydration was carried out using an ethanol gradient (75–100%). The slices were then boiled

in citrate buffer (0.01 M, pH 6.0) (AWI0206a, Abiowell) for antigen retrieval. 1% periodic acid was employed to inactivate the endogenous enzymes. The slices were incubated with antibodies of PD-L1 (1:200, ab238697, Abcam) overnight at 4 °C, and then incubated with 100  $\mu$ L of HRP-anti-Rabbit-IgG for 30 min at 37 °C. Following these steps, 100  $\mu$ L of diaminobenzidine (DAB) was added to slices and incubated for 5 min. The slices were counterstained with hematoxylin for 5 min, rinsed with distilled water, and returned to blue in PBS. Dehydration was carried out with an ethanol gradient (60–100%), 5 min for each level. Finally, the slices were clarified in xylene for 10 min and sealed with neutral gum for observation.

#### 2.7 16S rRNA Sequencing

DNA was extracted from fecal samples using a TIANamp Stool DNA Kit (#DP328-02, Tiangen, Beijing, China). PCR amplification and library construction were conducted using Phusion enzyme (K1031, APEX BIO, Houston, TX, USA) and the V3-V4 region primers (341F 5'-CCTACGGGNGGCWGCAG-3' and 805R 5'-GACTACHVGGGTATCTAATCC-3') of the 16S rRNA gene. An Illumina NovaSeq6000 instrument was used for paired-end (PE250) sequencing to collect raw data. Qiime 2 (2020.2) was used to conduct data quality control, calculate the  $\alpha$  diversity index, and measure relative abundance. Each Amplicon Sequence Variant/Operating Taxonomic Units (ASV/OUT) sequence was annotated by referring to the silva-132-99 database, and the corresponding species information and abundance distribution were obtained. R software 4.2.3 (University of Auckland, Auckland, New Zealand) (Venn Diagram package) and the Jvenn web page (<http://www.bioinformatics.com.cn/static/others/jvenn/example.html>) were used to analyze common and unique ASVs in groups. Linear Discriminant Analysis (LDA) Effect Size analysis (LefSe, <https://github.com/SegataLab/lefse>) was applied to evaluate the differential microbiota.

#### 2.8 Data Analysis

GraphPad Prism 8.0 (GraphPad Software Inc., San Diego, CA, USA) was applied for data analysis. All experimental data were expressed as mean  $\pm$  standard deviation (SD). One-way analysis of variance (one-way ANOVA) was applied to compare groups, and  $p < 0.05$  was considered statistically significant.

### 3. Results

#### 3.1 Combination Therapy Inhibited HCC Progression

To assess the impact of combination therapy on the progression of HCC, mice injected with the fourth generation of Hepal-6 cells were treated with quercetin both with and without coordinate injection of anti-PD-1 antibody. The liver tissues in the Model group exhibited obvious tumors, confirming the successful construction of the ortho-

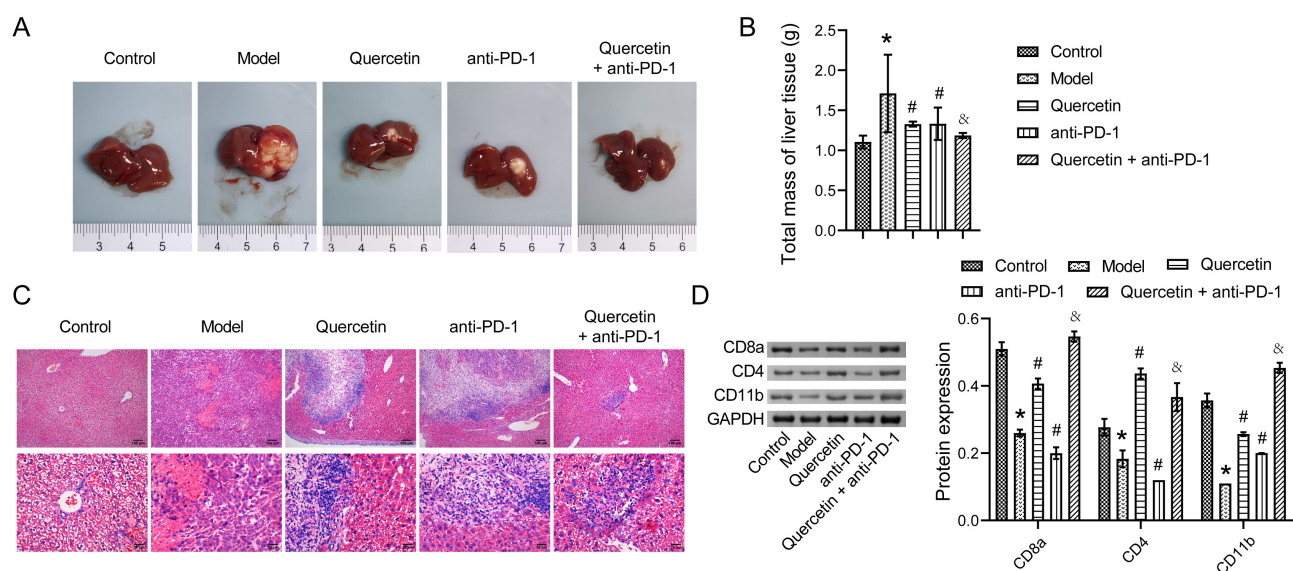


**Fig. 1. The combination therapy inhibited the progression of hepatocellular carcinoma (HCC).** (A) The distribution of tumors in liver tissues; (B) The total mass of liver tissues; (C) Hematoxylin and eosin (H&E) staining analysis of the pathological changes in liver tissues; (D) Western blot analysis of the expressions of CD8a, CD4, and CD11b in liver tissues. \*  $p < 0.05$  vs. Control, #  $p < 0.05$  vs. Model, &  $p < 0.05$  vs. Quercetin or anti-PD-1.

topically transplanted HCC model. Tumors in the liver tissues of mice were reduced when mice were treated with either quercetin or anti-PD-1 antibody alone. Combination therapy more effectively inhibited the growth of HCC than either monotherapy (Fig. 1A,B). Hematoxylin and eosin (H&E) staining of the liver tissues taken from different groups displayed that the liver cells of mice in the Control group were uniformly sized, neatly arranged, and without inflammatory infiltration. In the Model group, the volume of liver cells increased, nuclear staining deepened, and cell necrosis and fibrosis were observed. However, upon receiving combination therapy, the appearance of hepatocellular lesions was improved, and cell necrosis and inflammatory infiltration were significantly reduced (Fig. 1C). Western blot exhibited that the expressions of CD8a, CD4, and CD11b in liver tissues of the Model group were markedly downregulated compared to Control. Contrarily, combination therapy resulted in markedly increased expression of CD8a, CD4, and CD11b in liver tissues (Fig. 1D). Taken together, these findings indicated that combination therapy inhibited the progression of HCC.

### 3.2 Combination Therapy Regulated the Diversity of GM in Orthotopically Transplanted HCC Model Mice

To explore the impact of combination therapy on the diversity of GM in the orthotopically transplanted HCC model mice, 16S rRNA sequencing was carried out on mouse fecal samples. A rank-abundance curve demonstrated increased richness and evenness of GM in the Model group, but this decreased following combination therapy (Fig. 2A). As shown in the Venn diagram, the number of unique microorganisms in Control, Model, Quercetin, anti-

PD-1, and Quercetin+anti-PD-1 groups was 290, 266, 195, 195, and 242, respectively (Fig. 2B). Analysis of inter-group difference showed that the  $\alpha$  diversity index of the Model group was higher than that in the Control group, but the difference was not statistically significant. However, the  $\alpha$  diversity index was considerably reduced in mice that received combination therapy (Fig. 2C). At the phylum level, the GM principally consisted of *Bacteroidota*, *Firmicutes*, *Actinobacteria*, *Verrucomicrobiota*, *Proteobacteria*, *Campilobacterota*, *Desulfobacterota*, *Patescibacteria*, *Cyanobacteria*, *Deferribacterota*, and *Chloroflexi*. The abundance of *Firmicutes* was decreased but that of *Bacteroidota* increased in GM of mice in the Model group when compared to the Control group. However, the GM of mice in the Quercetin+anti-PD-1 antibody group displayed that the relative abundance of *Bacteroidota* decreased, while that of *Firmicutes*, *Actinobacteria*, and *Verrucomicrobiota* increased (Fig. 2D). At the genus level, the GM primarily included *Muribaculaceae*, *Lactobacillus*, *Lachnospiraceae\_NK4A136\_group*, *Dubosiella*, *Bacteroides*, *Akkermansia*, *Enterorhabdus*, *Alloprevotella*, *Blautia*, *Helicobacter*, *Alistipes*, *Lachnoclostridium*, *Bifidobacterium*, *Erysipelatoclostridium*, *Parabacteroides*, *Bacilli*, *Oscillospiraceae*, *Anaerotruncus*, and *Rikenellaceae*. The abundance of *Lactobacillus* and *Lachnospiraceae\_NK4A136\_group* decreased, but that of *Bacteroides* increased in the GM of mice in the Model group compared with that measured in the Control group. However, the GM of mice in the Quercetin+anti-PD-1 antibody group displayed that the abundance of *Muribaculaceae* decreased, while that of *Dubosiella* and *Akkerman-*

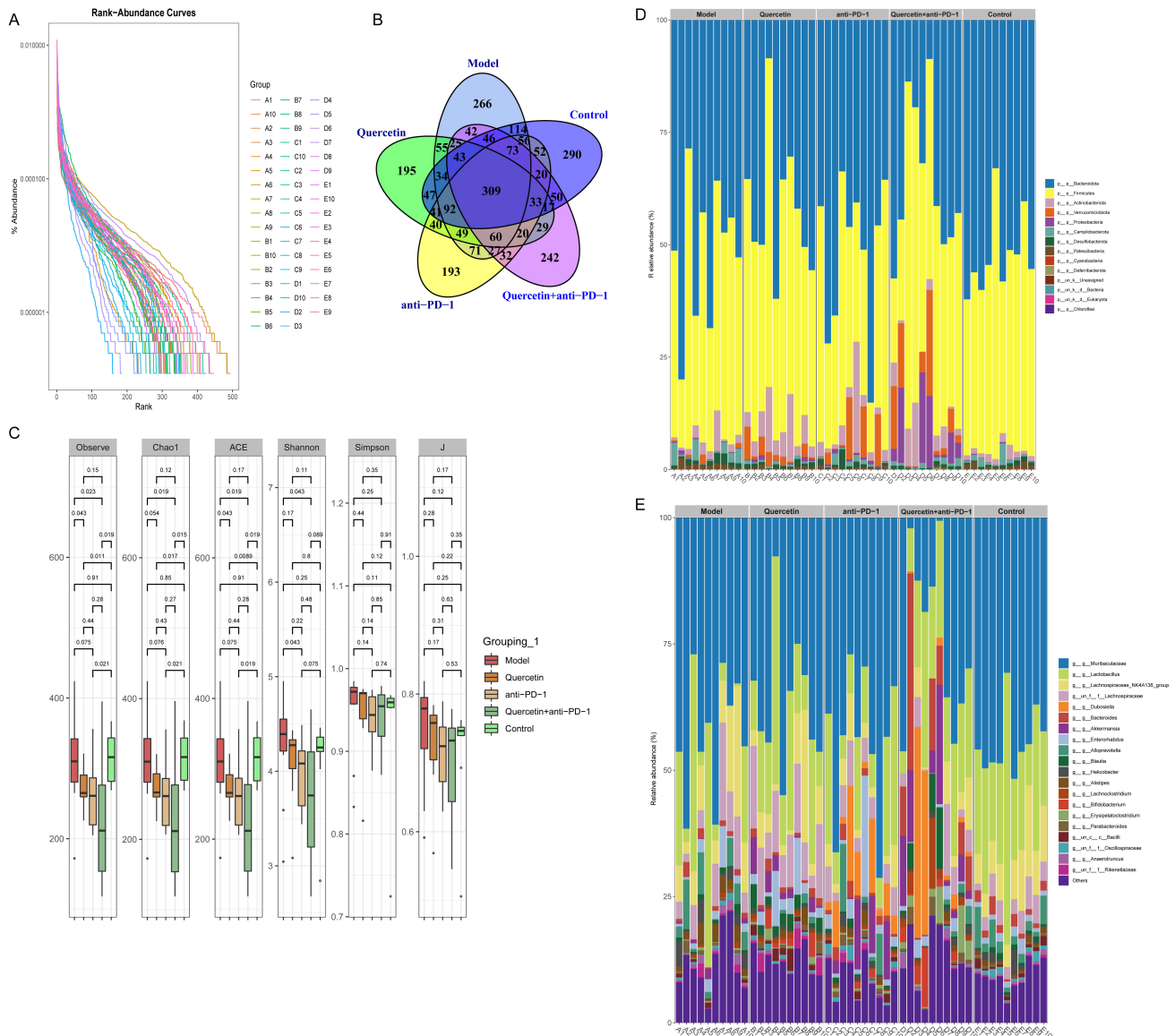


**Fig. 2. The combination therapy regulated the diversity of gut microbiota (GM) in orthotopically transplanted HCC model mice.** (A) Rank-abundance curve of the richness and evenness of GM. (B) Venn diagram of the number of GM. (C) Analysis of  $\alpha$  diversity index. (D,E) Analysis of relative species abundance at phylum and genus level.

*sia* increased (Fig. 2E). These results proved that the combination therapy influenced the diversity of mouse GM in the orthotopically transplanted HCC model.

### 3.3 The Combination Therapy Regulated the Difference of GM in Orthotopically Transplanted HCC Model Mice

We next investigated the effect of combination therapy on the difference in GM in the HCC model. Difference analysis between groups indicated that *Clostridia\_UCG-014*, *Lachnospiraceae\_UCG-006*, *Monoglobus*, and *Akkermansia* were enriched in the intestine of mice in the Model group. *Bifidobacterium*, *Atopobiaceae*, and *Faecalibulum* were enriched in the intestine of mice in the Quercetin group (Fig. 3A). Subsequently, the phylum-level analysis indicated that *Campilobacterota*, *Deferribacterota*, *Patescibac-*

*teria*, *Actinobaciota*, *Proteobacteria*, and *Verrucomicrobiota* were the key differential GM. *Campilobacterota* and *Patescibacteria* were enriched in the intestine of mice in both Control and Model groups. *Deferribacterota*, *Actinobaciota*, *Proteobacteria*, and *Verrucomicrobiota* were enriched in the intestine of mice in the Quercetin+anti-PD-1 group (Fig. 3B). These results proved that the combination therapy regulated GM variation in HCC model.

### 3.4 The Combination Therapy Regulated the Immunity of Orthotopically Transplanted HCC Model Mice

To explore the impact of combination therapy on the immunity of the orthotopically transplanted HCC model mice, cytokine concentrations were examined using enzyme-linked immunosorbent assay (ELISA) and Western

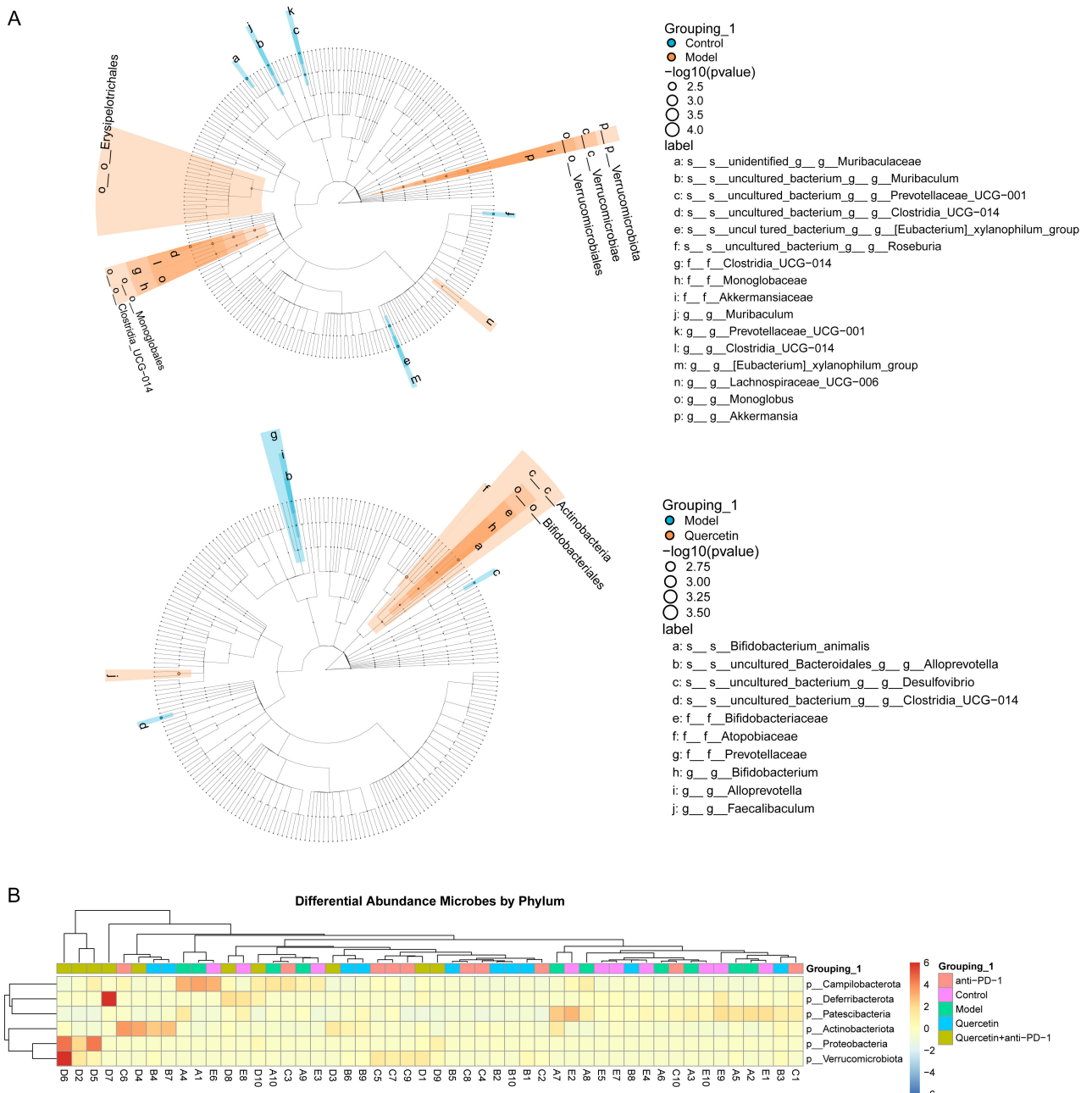


**Fig. 3. The combination therapy regulated the difference of GM in orthotopically transplanted HCC model mice. (A)** Lefse analysis of differential GM between groups. **(B)** Heatmap of the differential GM abundance between groups at the phylum level.

blot. In the blood of Model mice, the levels of IL-6 and IL-4 increased, while those of IL-10 and IFN- $\gamma$  decreased. In mice receiving combination therapy, the levels of IL-6 and IL-4 were lower, but those of IL-10 and IFN- $\gamma$  were higher than that in the Quercetin or anti-PD-1 group (Fig. 4A). The levels of GM-CSF and G-CSF were increased in the liver tissues of the Model group when compared to the Control group. However, both GM-CSF and G-CSF markedly decreased in the Quercetin or anti-PD-1 group. In addition, compared with the therapy of Quercetin or anti-PD-1, combination therapy produced a better inhibitory effect on the

levels of GM-CSF and G-CSF (Fig. 4B). Next, we discovered that TLR4 expression was markedly upregulated in the Model group compared to the Control group, and the phosphorylation levels of both I $\kappa$ B $\alpha$  and p65 were increased. However, following combination therapy, TLR4 expression was downregulated, and the phosphorylation of I $\kappa$ B $\alpha$  and p65 was reduced (Fig. 4C). Additionally, the immunotherapy marker PD-L1 was highly expressed in the liver tissues of the Model group as determined by immunohistochemistry (IHC) staining analysis, however, its expression was suppressed in the Quercetin+anti-PD-1 group

(Fig. 4D). These results confirmed that combination therapy regulated the immunity of the orthotopically transplanted HCC model mice.

### 3.5 The Combination Therapy Regulated Macrophage Immunity in Orthotopically Transplanted HCC Model Mice

Finally, to explore the underlying mechanism of combination therapy in regulating macrophage immunity in orthotopically transplanted HCC model mice, RT-qPCR was conducted to analyze macrophage-related gene expressions. M1 macrophage-related genes, including *IL-6*, *IL-12a*, *IL-1 $\beta$* , and *TNF- $\alpha$* , were highly expressed in the liver tissues of the Model group, whereas their expression levels were suppressed in those of the Quercetin+anti-PD-1 group (Fig. 5A). Moreover, the expressions of M2 macrophage-related genes, including *Arg-1*, *IL-10*, *TGF- $\beta$* , and *MMP-9*, were inhibited in the liver tissues of the Model group. However, combination therapy overcame this inhibitory effect to a large extent, resulting in the increased expression of *Arg-1*, *IL-10*, *TGF- $\beta$* , and *MMP-9* (Fig. 5B). These findings indicated that the combination therapy regulated macrophage immunity in orthotopically transplanted HCC model mice.

## 4. Discussion

Natural compounds derived from TCM, including quercetin, are therapeutic for HCC but without side effects [19]. In addition, immune checkpoint blockade immunotherapy based on PD-1/PD-L1 has recently demonstrated encouraging outcomes in HCC treatment [9]. Multiple studies have proved that combination therapies based on quercetin or PD-1 inhibitors can effectively limit HCC progression [20,21]. However, the exact mechanism of combination therapy for HCC remains to be explored. Herein, we have provided data obtained from mice orthotopically transplanted with HCC cells and treated with quercetin in combination with and without anti-PD-1 antibody. This study confirmed that combination therapy reshaped the TME of orthotopically transplanted HCC model mice by regulating both GM and macrophage immunity (Fig. 6).

The anti-tumor effects of quercetin in HCC models have been demonstrated in both *in vitro* and *in vivo* studies [13]. After quercetin treatment in mice, liver tissue injury and inflammatory infiltration were reduced in mice [22]. Here, H&E staining showed that cell necrosis, fibrosis, and inflammatory infiltration were reduced in the liver tissues of mice receiving combination therapy, thus the progression of HCC was significantly inhibited. The results also presented that combination therapy of quercetin and anti-PD-1 antibody had a stronger anti-cancer effect than either quercetin or anti-PD-1 antibody alone. It is well-established that TME plays a critical role in tumor occurrence and progression [23]. Besides, PD-1 inhibitors work by activating tumor infiltration of lymphocytes to inhibit tumor growth [24,25]. Here, Western blot displayed low

expressions of CD8a, CD4, and CD11b in liver tissues of HCC mice, which were considerably elevated in response to combination therapy. This suggested that combination therapy could restore immune recognition and attack within the TME, thereby enhancing anti-tumor immune response. These results further proved that the combination therapy limited further progression of HCC by activating an anti-tumor immune response.

Increasingly, studies have illustrated the participation of GM in the occurrence and progression of HCC through the engagement of the gut-liver axis. Hence, reshaping the homeostasis of GM holds significant potential to delay HCC progression [7]. Clinical studies on HCC patients found that the relative abundance of *Firmicutes* in the GM is significantly decreased, while that of *Bacteroidetes* is significantly increased relative to healthy controls [26]. Moreover, the *Firmicutes/Bacteroidetes* ratio serves as an ecological imbalance indicator of GM. Here, the  $\alpha$  diversity of GM in HCC mice was not significantly changed, but its structure and species were altered, possibly due to the limited number of samples evaluated. The disrupted homeostasis of gut microbiota in mice with HCC was reflected by a decrease in the relative abundance of *Firmicutes* and an increase in *Bacteroides* at the phylum level. However, the combination therapy decreased the abundance of *Bacteroidetes* but increased that of *Firmicutes*, *Actinobacteria*, and *Verrucomicrobiota*. Further analysis revealed that the relative abundance of *Lactobacillus* and *Lachnospira* decreased, while that of *Bacteroides* increased in the intestines of HCC mice. The combination therapy significantly improved the imbalance of GM and boosted the relative abundance of *Dubosiella* and *Akkermansia*. Numerous studies have shown that the diversity and dynamic alterations observed within the GM correlate with the efficacy of anti-PD-1 in HCC treatment [9]. Additionally, studies have revealed that the GM of HCC patients responding to anti-PD-1 treatment undergoes a significant enrichment of *Akkermansia* and *Ruminococcus* [9]. *Akkermansia* has been regarded as a beneficial bacterium in improving anti-tumor immunity and more effectively controlling the growth of tumors *in vivo* [27]. Taken together, combination therapy improved GM imbalance to enhance the efficiency of HCC treatment.

In HCC, TAMs are crucial components of TME and are intimately linked to poor patient prognosis [28]. Studies on HCC show that upregulated expressions of both IL-4 and IL-6 are related to TAMs infiltration and HCC metastasis [29]. Others have discovered that apigenin can induce apoptosis in HCC cells by suppressing IL-4 expression. In addition, MiR-98 can inhibit HCC progression by increasing IL-10 expression and inhibiting TAMs [30]. IFN- $\gamma$  primarily participates in promoting the formation of M1-type macrophages, activating immunity, and suppressing tumor progression [31]. Here, the expressions of IL-4 and IL-6 were downregulated while those of IL-10 and IFN- $\gamma$  were upregulated in HCC mice treated with combination

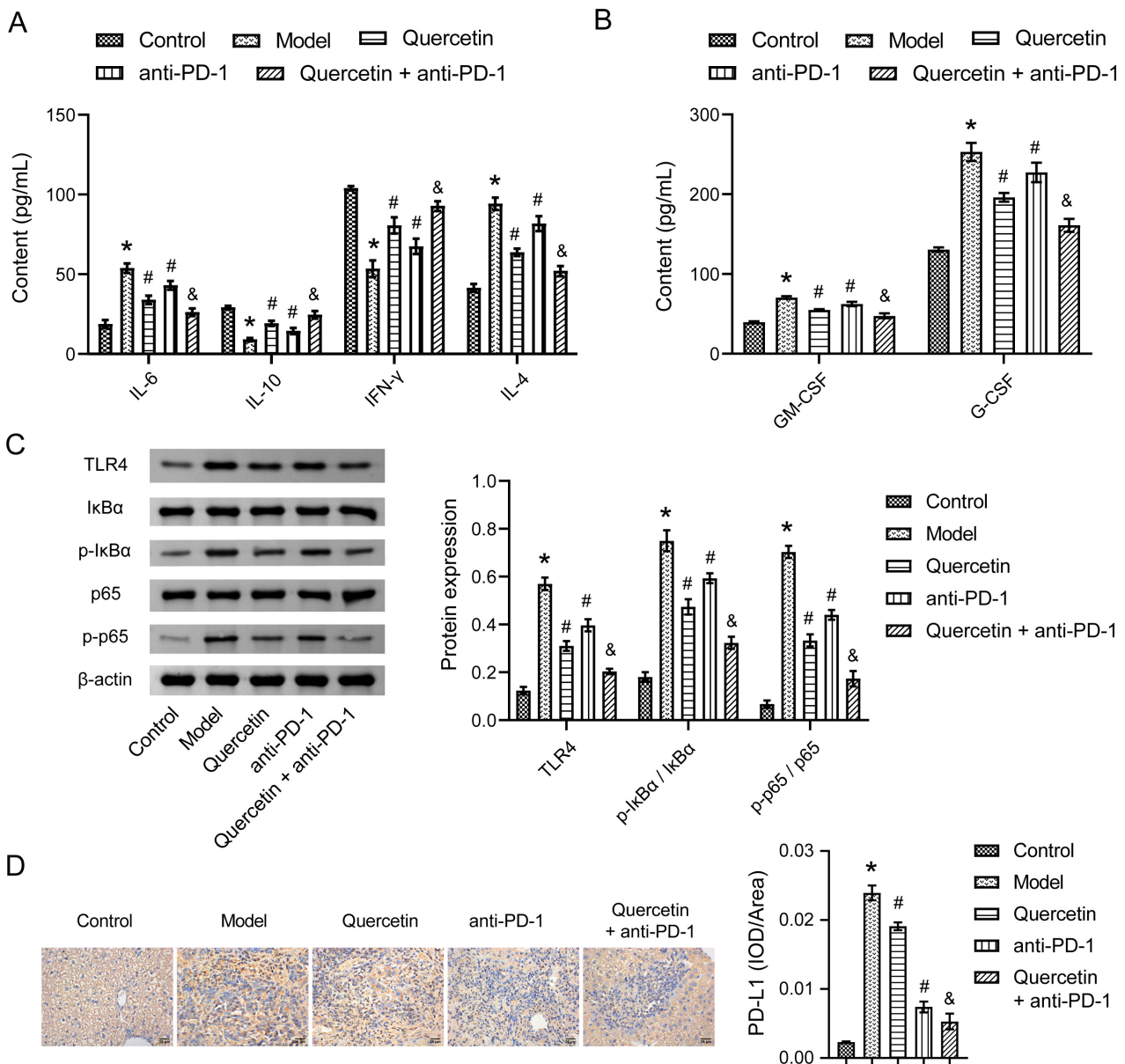


**Fig. 4. The combination therapy regulated the immunity of orthotopically transplanted HCC model mice.** (A) The levels of interleukin (IL)-6, IL-10, interferon (IFN)- $\gamma$ , and IL-4 in blood were determined by enzyme-linked immunosorbent assay (ELISA). (B) The levels of granulocyte-macrophage colony-stimulating factor (GM-CSF) and granulocyte colony-stimulating factor (G-CSF) in liver tissues were assessed by ELISA. (C) The expressions of TLR4, I $\kappa$ B $\alpha$ , p-I $\kappa$ B $\alpha$ , p65, and p-p65 in liver tissues were analyzed by Western blot. (D) programmed cell death 1 ligand 1 (PD-L1) expression in liver tissues was characterized by IHC staining. \*  $p < 0.05$  vs. Control, #  $p < 0.05$  vs. Model, &  $p < 0.05$  vs. Quercetin or anti-PD-1.

therapy, suggesting that combination therapy could significantly enhance the immune response in TME. A previous study has reported that high expression of GM-CSF and G-CSF can accelerate the formation of tumor microvessels, as well as alter the TME and promote tumor growth and metastasis [32]. Moreover, patients with chronic liver disease can be effectively treated using GM-CSF and G-CSF-neutralizing antibodies [33]. Consistent with these findings, upon combination therapy, the expressions of GM-

CSF and G-CSF in liver tissues of HCC mice were significantly downregulated, which was attributed to the outstanding anti-inflammatory activity displayed by quercetin [34]. Moreover, we discovered that the combination therapy inhibited TLR4 expression and phosphorylation levels of p-I $\kappa$ B $\alpha$  and p65. Studies have investigated that blocking the TLR4/STAT3 signaling pathway can effectively suppress the migration of HCC cells [35]. Additional studies have documented that further HCC progression can be

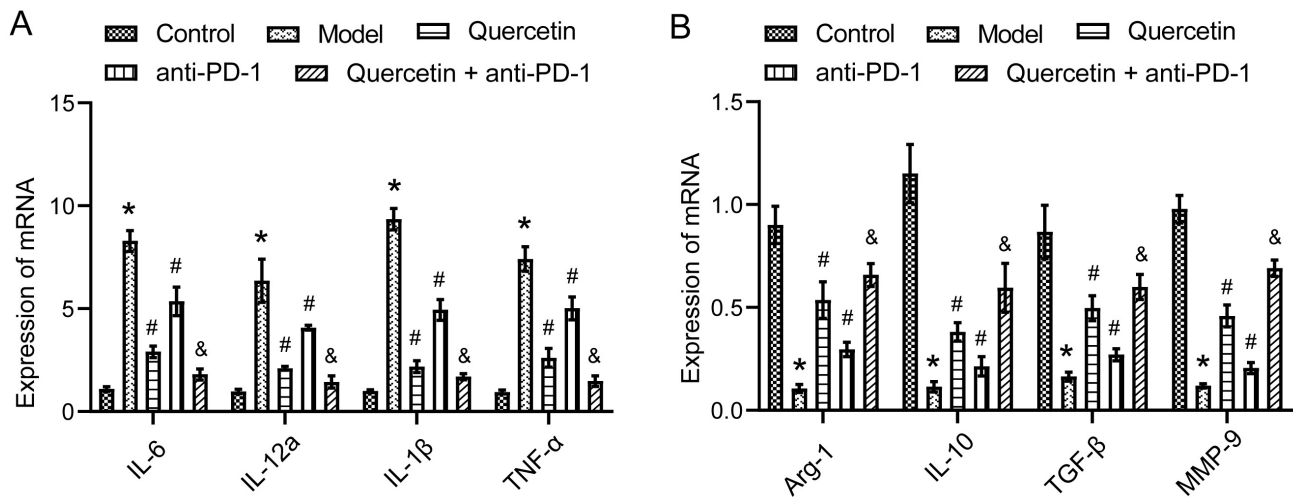


**Fig. 5. The combination therapy regulated macrophage immunity in orthotopically transplanted HCC model mice.** (A) The expressions of M1 macrophage-related genes *IL-6*, *IL-12a*, *IL-1β*, and *TNF-α* in liver tissues were quantified by RT-qPCR. (B) The expressions of M2 macrophage-related genes *Arg-1*, *IL-10*, *TGF-β*, and *MMP-9* in liver tissues were detected by RT-qPCR. \*  $p < 0.05$  vs. Control, #  $p < 0.05$  vs. Model, &  $p < 0.05$  vs. Quercetin or anti-PD-1.

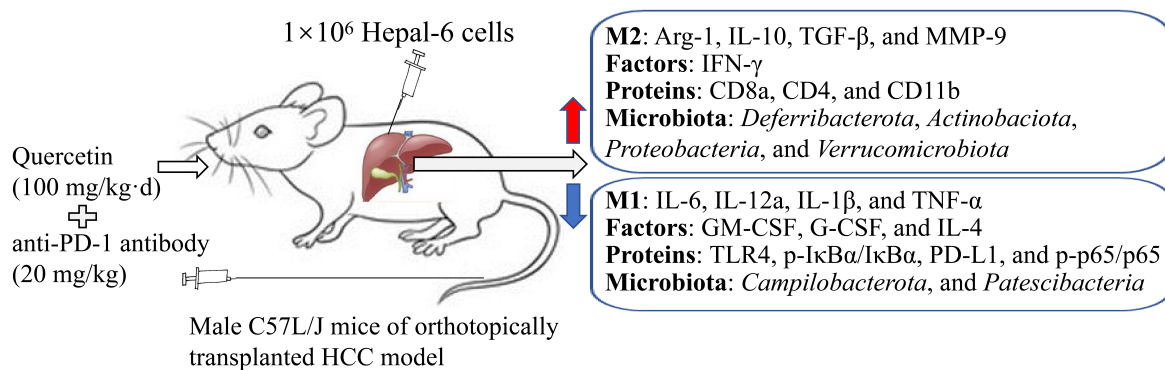


**Fig. 6. The combination therapy of quercetin and anti-PD-1 antibody in HCC mice was achieved through the regulation of GM and macrophage immunity.**

hindered by inhibiting the phosphorylation of p-IκBα and p65 within the NF-κB signaling pathway [36]. IHC staining of PD-L1 expression in liver tissues determined that combination therapy significantly inhibited PD-L1 expression in HCC mice, and this was related to the effect of quercetin on the interaction of PD-1/PD-L1 as well as the effect of anti-PD-1 antibody on the binding site of PD-1 [15,37]. M1-type macrophages may play a role in promoting tumors by secreting IL-1β and promoting PD-L1 expression in HCC cells [38]. Interestingly, the combination therapy significantly downregulated the expression levels of M1 macrophage-related genes and upregulated that of M2 macrophage-related genes. Thus, the combination therapy reshaped the TME of HCC by regulating macrophage immunity.

This study only investigated the combination therapy of quercetin and PD-1 inhibitor for HCC. In TCM, many components exhibit therapeutic effects on HCC. In the fu-

ture, the combined therapeutic effects of different active components with PD-1 inhibitors can be explored, and their specific therapeutic mechanisms of action through modulating the gut-liver axis can be elucidated. This will provide a theoretical basis for investigating the pathogenesis of HCC as well as developing new drugs.

## 5. Conclusions

Here, we found that combination therapy reshaped the TME of HCC mice. The therapeutic effect was paralleled by the regulation of the GM and macrophage immunity. This study suggested that TCM ingredients in combination with PD-1 inhibitors could be a potential new strategy for HCC treatment.

## Availability of Data and Materials

Data can be provided upon request.

## Author Contributions

RW designed the research study. RW, JX, TZ, ST, YW, ZZ and ZH performed the research. RW and JX analyzed the data. RW wrote the manuscript. All authors contributed to editorial changes in the manuscript. All authors read and approved the final manuscript. All authors have participated sufficiently in the work and agreed to be accountable for all aspects of the work.

## Ethics Approval and Consent to Participate

The animal experiment was approved by the Ethics Committee (Hidden by assistant editor according to double-blind principle) (No. ZYFY20210320).

## Acknowledgment

Not applicable.

## Funding

This research was funded by Youth program of Natural Science Foundation of Hunan Province, grant number 2021JJ40407; Youth project of Hunan Administration of traditional Chinese Medicine, grant number 202101; and Outstanding youth project of Hunan Education Department, grant number 20B451.

## Conflict of Interest

The authors declare no conflict of interest.

## References

- [1] Frager SZ, Schwartz JM. Hepatocellular carcinoma: epidemiology, screening, and assessment of hepatic reserve. *Current Oncology (Toronto, Ont.)*. 2020; 27: S138–S143.
- [2] Forner A, Reig M, Bruix J. Hepatocellular carcinoma. *Lancet (London, England)*. 2018; 391: 1301–1314.
- [3] Critelli R, Milosa F, Faillaci F, Condello R, Turola E, Marzi L, *et al.* Microenvironment inflammatory infiltrate drives growth speed and outcome of hepatocellular carcinoma: a prospective clinical study. *Cell Death & Disease*. 2017; 8: e3017.
- [4] Xu G, Feng D, Yao Y, Li P, Sun H, Yang H, *et al.* Listeria-based hepatocellular carcinoma vaccine facilitates anti-PD-1 therapy by regulating macrophage polarization. *Oncogene*. 2020; 39: 1429–1444.
- [5] Rizzo A, Ricci AD, Di Federico A, Frega G, Palloni A, Tavolari S, *et al.* Predictive Biomarkers for Checkpoint Inhibitor-Based Immunotherapy in Hepatocellular Carcinoma: Where Do We Stand? *Frontiers in Oncology*. 2021; 11: 803133.
- [6] Rizzo A, Cusmai A, Gadaleta-Caldarola G, Palmiotti G. Which role for predictors of response to immune checkpoint inhibitors in hepatocellular carcinoma? *Expert Review of Gastroenterology & Hepatology*. 2022; 16: 333–339.
- [7] Yu LX, Schwabe RF. The gut microbiome and liver cancer: mechanisms and clinical translation. *Nature Reviews. Gastroenterology & Hepatology*. 2017; 14: 527–539.
- [8] Rezasoltani S, Yadegar A, Asadzadeh Aghdaei H, Reza Zali M. Modulatory effects of gut microbiome in cancer immunotherapy: A novel paradigm for blockade of immune checkpoint inhibitors. *Cancer Medicine*. 2021; 10: 1141–1154.
- [9] Zheng Y, Wang T, Tu X, Huang Y, Zhang H, Tan D, *et al.* Gut microbiome affects the response to anti-PD-1 immunotherapy in patients with hepatocellular carcinoma. *Journal for Immunotherapy of Cancer*. 2019; 7: 193.
- [10] Viscardi G, Tralongo AC, Massari F, Lambertini M, Mollica V, Rizzo A, *et al.* Comparative assessment of early mortality risk upon immune checkpoint inhibitors alone or in combination with other agents across solid malignancies: a systematic review and meta-analysis. *European Journal of Cancer (Oxford, England: 1990)*. 2022; 177: 175–185.
- [11] Di Federico A, Rizzo A, Carloni R, De Giglio A, Bruno R, Ricci D, *et al.* Atezolizumab-bevacizumab plus Y-90 TARE for the treatment of hepatocellular carcinoma: preclinical rationale and ongoing clinical trials. *Expert Opinion on Investigational Drugs*. 2022; 31: 361–369.
- [12] Zhao X, Wang J, Deng Y, Liao L, Zhou M, Peng C, *et al.* Quercetin as a protective agent for liver diseases: A comprehensive descriptive review of the molecular mechanism. *Phytotherapy Research: PTR*. 2021; 35: 4727–4747.
- [13] Fernández-Palanca P, Fondevila F, Méndez-Blanco C, Tuñón MJ, González-Gallego J, Mauriz JL. Antitumor Effects of Quercetin in Hepatocarcinoma *In Vitro* and *In Vivo* Models: A Systematic Review. *Nutrients*. 2019; 11: 2875.
- [14] Reyes-Avendaño I, Reyes-Jiménez E, González-García K, Pérez-Figueroa DC, Baltiérrez-Hoyos R, Tapia-Pastrana G, *et al.* Quercetin Regulates Key Components of the Cellular Microenvironment during Early Hepatocarcinogenesis. *Antioxidants (Basel, Switzerland)*. 2022; 11: 358.
- [15] Jing L, Lin J, Yang Y, Tao L, Li Y, Liu Z, *et al.* Quercetin inhibiting the PD-1/PD-L1 interaction for immune-enhancing cancer chemopreventive agent. *Phytotherapy Research: PTR*. 2021; 35: 6441–6451.
- [16] Li Y, Shi X, Zhang J, Zhang X, Martin RCG. Hepatic protection and anticancer activity of curcuma: a potential chemopreventive strategy against hepatocellular carcinoma. *International Journal of Oncology*. 2014; 44: 505–513.
- [17] Wang G, Zhang J, Liu L, Sharma S, Dong Q. Quercetin potentiates doxorubicin mediated antitumor effects against liver cancer through p53/Bcl-xl. *PLoS ONE*. 2012; 7: e51764.
- [18] Ho TTB, Nasti A, Seki A, Komura T, Inui H, Kozaka T, *et al.* Combination of gemcitabine and anti-PD-1 antibody enhances the anticancer effect of M1 macrophages and the Th1 response in a murine model of pancreatic cancer liver metastasis. *Journal for Immunotherapy of Cancer*. 2020; 8: e001367.
- [19] Yan J, Nie Y, Luo M, Chen Z, He B. Natural Compounds: A Potential Treatment for Alcoholic Liver Disease? *Frontiers in Pharmacology*. 2021; 12: 694475.
- [20] Zou H, Zheng YF, Ge W, Wang SB, Mou XZ. Synergistic Antitumor Effects of Quercetin and Oncolytic Adenovirus expressing TRAIL in Human Hepatocellular Carcinoma. *Scientific Reports*. 2018; 8: 2182.
- [21] Liu BJ, Gao S, Zhu X, Guo JH, Kou FX, Liu SX, *et al.* Real-world study of hepatic artery infusion chemotherapy combined with anti-PD-1 immunotherapy and tyrosine kinase inhibitors for advanced hepatocellular carcinoma. *Immunotherapy*. 2021; 13: 1395–1405.
- [22] Wang J, Miao M, Zhang Y, Liu R, Li X, Cui Y, *et al.* Quercetin ameliorates liver injury induced with Tripterygium glycosides by reducing oxidative stress and inflammation. *Canadian Journal of Physiology and Pharmacology*. 2015; 93: 427–433.
- [23] Quail DF, Joyce JA. Microenvironmental regulation of tumor progression and metastasis. *Nature Medicine*. 2013; 19: 1423–1437.
- [24] Ferris ST, Durai V, Wu R, Theisen DJ, Ward JP, Bern MD, *et al.* cDC1 prime and are licensed by CD4<sup>+</sup> T cells to induce antitumor immunity. *Nature*. 2020; 584: 624–629.
- [25] Siddiqui I, Schaeuble K, Chennupati V, Fuertes Marraco SA, Calderon-Copete S, Pais Ferreira D, *et al.* Intratumoral

- Tcf1<sup>+</sup>PD-1<sup>+</sup>CD8<sup>+</sup> T Cells with Stem-like Properties Promote Tumor Control in Response to Vaccination and Checkpoint Blockade Immunotherapy. *Immunity*. 2019; 50: 195–211.e10.
- [26] Zeng Y, Chen S, Fu Y, Wu W, Chen T, Chen J, *et al.* Gut microbiota dysbiosis in patients with hepatitis B virus-induced chronic liver disease covering chronic hepatitis, liver cirrhosis and hepatocellular carcinoma. *Journal of Viral Hepatitis*. 2020; 27: 143–155.
- [27] Li W, Deng Y, Chu Q, Zhang P. Gut microbiome and cancer immunotherapy. *Cancer Letters*. 2019; 447: 41–47.
- [28] Lu C, Rong D, Zhang B, Zheng W, Wang X, Chen Z, *et al.* Current perspectives on the immunosuppressive tumor microenvironment in hepatocellular carcinoma: challenges and opportunities. *Molecular Cancer*. 2019; 18: 130.
- [29] Jiang J, Wang GZ, Wang Y, Huang HZ, Li WT, Qu XD. Hypoxia-induced HMGB1 expression of HCC promotes tumor invasiveness and metastasis via regulating macrophage-derived IL-6. *Experimental Cell Research*. 2018; 367: 81–88.
- [30] Li L, Sun P, Zhang C, Li Z, Zhou W. MiR-98 suppresses the effects of tumor-associated macrophages on promoting migration and invasion of hepatocellular carcinoma cells by regulating IL-10. *Biochimie*. 2018; 150: 23–30.
- [31] Gordon S, Martinez FO. Alternative activation of macrophages: mechanism and functions. *Immunity*. 2010; 32: 593–604.
- [32] Phan VT, Wu X, Cheng JH, Sheng RX, Chung AS, Zhuang G, *et al.* Oncogenic RAS pathway activation promotes resistance to anti-VEGF therapy through G-CSF-induced neutrophil recruitment. *Proceedings of the National Academy of Sciences of the United States of America*. 2013; 110: 6079–6084.
- [33] Tan-Garcia A, Lai F, Sheng Yeong JP, Irac SE, Ng PY, Msallam R, *et al.* Liver fibrosis and CD206<sup>+</sup> macrophage accumulation are suppressed by anti-GM-CSF therapy. *JHEP Reports: Innovation in Hepatology*. 2019; 2: 100062.
- [34] Kim YJ, Park W. Anti-Inflammatory Effect of Quercetin on RAW 264.7 Mouse Macrophages Induced with Polyinosinic-Polycytidylic Acid. *Molecules (Basel, Switzerland)*. 2016; 21: 450.
- [35] Yao RR, Li JH, Zhang R, Chen RX, Wang YH. M2-polarized tumor-associated macrophages facilitated migration and epithelial-mesenchymal transition of HCC cells via the TLR4/STAT3 signaling pathway. *World Journal of Surgical Oncology*. 2018; 16: 9.
- [36] Cao J, Qiu J, Wang X, Lu Z, Wang D, Feng H, *et al.* Identification of microRNA-124 in regulation of Hepatocellular carcinoma through BIRC3 and the NF- $\kappa$ B pathway. *Journal of Cancer*. 2018; 9: 3006–3015.
- [37] Li W, Kim TI, Kim JH, Chung HS. Immune Checkpoint PD-1/PD-L1 CTLA-4/CD80 are Blocked by *Rhus verniciflua* Stokes and its Active Compounds. *Molecules (Basel, Switzerland)*. 2019; 24: 4062.
- [38] Zong Z, Zou J, Mao R, Ma C, Li N, Wang J, *et al.* M1 Macrophages Induce PD-L1 Expression in Hepatocellular Carcinoma Cells Through IL-1 $\beta$  Signaling. *Frontiers in Immunology*. 2019; 10: 1643.